Published in final edited form as:
Heart Rhythm. 2010 September ; 7(9): 1207–1215. doi:10.1016/j.hrthm.2010.06.018.

Different characteristics of complex fractionated atrial electrograms in acute paroxysmal versus long-standing persistent atrial fibrillation

Edward J. Ciaccio, PhD, **Angelo B. Biviano, MD**, **William Whang, MD**, **Alok Gambhir, MD, PhD**, and **Hasan Garan, MD**
Department of Medicine, Division of Cardiology, Columbia University Medical Center, New York, New York

Abstract

BACKGROUND—Complex fractionated atrial electrograms (CFAEs) may represent a phenomenon associated with sources of atrial fibrillation (AF) and are being used increasingly as targets of catheter ablation. However, current methods have limited efficacy for characterizing CFAEs important to substrate arrhythmogenicity and do not measure electrogram morphology.

OBJECTIVE—The purpose of this study was to develop a methodology for quantifying the degree of morphologic heterogeneity in CFAE deflections, and to determine whether there are differences in this measurement between paroxysmal and persistent AF patients.

METHODS—Two successive bipolar CFAEs of length 8.4 seconds each were acquired during AF from two sites each at the ostia of the four pulmonary veins (PVs) and from the anterior and posterior left atrial free wall in patients with paroxysmal AF (N =10) and long-standing persistent AF (N = 10). Extrinsic and intrinsic features of electrogram shape were used to characterize fractionation in CFAE sequences. The extrinsic parameters were the amplitude, upslope, downslope, and width of each deflection. The intrinsic parameter was the voltage profile as characterized by the sum of absolute values. These measurements were compared to the mean interval between CFAE deflections, a standard fractionation indicator.

RESULTS—The variability of intrinsic/extrinsic morphologic parameters was higher in paroxysmal than persistent AF at the left superior PV ($P \leq .003$), the posterior left atrial free wall, anterior left atrial free wall, left inferior PV, and right superior PV ($P < .05$ for most parameters), and the right inferior PV (not significant). Mean CFAE deflection intervals were longer at all locations in paroxysmal AF but were significant only at the left superior PV and posterior left atrial free wall ($P < .05$). Quantitative morphologic parameters were not well correlated with dominant frequency ($r^2 < 0.32$); thus, our new measures are robust to changes in activation rate.

CONCLUSION—A novel method for quantifying CFAEs, independent of activation rate, has been developed. The method demonstrates greater significance in the difference between CFAE

Address reprint requests and correspondence: Dr. Edward J. Ciaccio, HP804-Medicine, Columbia University, 180 Fort Washington Avenue, New York, New York 10032. ciaccio@columbia.edu.

morphology in paroxysmal and long-standing AF compared with mean interval between CFAE deflections. The differences identified suggest that CFAE morphology may evolve as AF persists.

Keywords

Atrial fibrillation; Fractionation; Left atrium

Introduction

Complex fractionated atrial electrograms (CFAEs) have been commonly recorded during atrial fibrillation (AF), but their underlying role in the mechanism of AF has not been clearly defined.[1] Clinical studies have suggested that CFAEs may represent sources or sites necessary for maintenance and perpetuation of AF.[2,3] However, CFAEs recorded during acute AF in patients with clinical paroxysmal AF and those recorded during persistent long-standing AF may represent a different underlying phenomenon. Assuming the presence of such possible differences in the genesis of CFAE formation in paroxysmal versus long-standing AF, we hypothesized that detectable and quantifiable differences exist, specifically in signal shape, which may reflect differences in underlying mechanisms between these two types of AF. To detect such differences, we developed novel methodologies for quantifying the degree of morphologic heterogeneity in CFAE components that characterize the electrogram morphology of CFAEs. Our study shows that such quantifiable and reproducible differences do indeed exist in CFAE patterns between acutely induced AF and persistent long-standing AF.

Methods

Clinical data and electrophysiologic procedure

Atrial electrograms manifesting CFAEs were recorded in a series of 20 patients referred to the Columbia University Medical Center for catheter ablation of AF. Ten patients had a history of paroxysmal AF, and 10 had long-standing persistent AF. None of the patients had been treated with amiodarone, and all other antiarrhythmic drugs had been discontinued for at least five half-lives before the day of the procedure. Other clinical and echocardiographic parameters are listed in Table 1. Multipolar electrode catheters were placed in the right atrium and coronary sinus, and a steerable 3.5-mm externally irrigated radiofrequency ablation catheter (Biosense Webster, Inc., Diamond Bar, CA, USA) was placed in the left atrium via transseptal puncture. Complete left atrial electroanatomic mapping was performed during AF to identify CFAE sites. In all patients with clinical long-standing AF, the underlying cardiac rhythm was AF in the cardiac electrophysiology laboratory, and as best as we could ascertain from all available records, AF had been present without interruption for 1 to 9 years (Table 1). In patients with paroxysmal AF, the frequency of episodes varied from 3 to 7 per year, and the baseline cardiac rhythm was sinus in all 10. Acute AF was repeatedly induced in the laboratory by rapid right atrial or coronary sinus pacing, until at least one AF episode lasted longer than 10 minutes. Electrically induced AF was allowed to persist for at least 10 minutes prior to any data collection. Bipolar CFAE recordings were obtained over an approximately 30-second period, and CFAE recording sites were marked on the three-dimensional CARTO maps (Biosense Webster). Recording

sites manifesting CFAE for shorter periods of time were not used for analysis in this study. CFAE was defined as high-frequency (cycle length ≤100 ms) signals with multiple (>3) positive or negative deflections or continuous electrical activity with no obvious isoelectric baseline.[4] Only signals that were identified by two cardiac electrophysiologists to be CFAEs using these criteria were included in the analysis. One cardiac electrophysiologist recorded the data in the cardiac electrophysiology laboratory. The second electrophysiologist who validated the CFAEs and selected the recording segments to be analyzed was blinded to patient identity, type of AF, and recording site. CFAE recordings over 16.8 seconds in duration were obtained from two sites in each patient at each of the ostia of the pulmonary veins (left superior pulmonary vein [LSPV], left inferior pulmonary vein [LIPV], right superior pulmonary vein [RSPV], right inferior pulmonary vein [RIPV]) and from the posterior and anterior left atrial free wall. The PV sites were less than 1 cm outside the ostia, determined by multiple criteria including three-dimensional CARTO software and intracardiac ultrasound. From each of these recordings, two consecutive 8.4-second CFAE sequences (8,192 sample points at 977-Hz sampling rate) were extracted and analyzed to assess the reproducibility and short-time temporal stability of our fractionation measures. A total of 480 CFAE sequences (2 consecutive sequences × 2 sites × 6 anatomic locations × 20 patients), each of 8.4-second duration, were included in the analysis. All electrogram recordings were obtained at the same gain during sustained AF prior to any ablation. To ensure sufficient electrode contact, the electrode tip icon on the three-dimensional CARTO map, fluoroscopic location, and impedance data were assessed at each recording site.

Using standard settings, all signals were filtered in hardware at acquisition to remove baseline drift and high-frequency noise (first-order filter passband 30–500 Hz). The electrograms were then sampled at 977 Hz and stored. Although the low-pass corner of 500 Hz is slightly greater than the Nyquist frequency, to prevent further distortion, software filters were not used at the inputs. The digitized signals were analyzed using computer programs developed by the authors. Retrospective analysis of electrograms was approved by the Institutional Review Board at Columbia University Medical Center. Because our analysis was retrospective, it did not affect catheter ablation treatment of the patients, which was performed based on the clinical protocols used in our laboratory and determined by the attending electrophysiologist. Specifically, CFAEs recorded in patients with paroxysmal AF were not used to guide catheter ablation, and CFAEs were not recorded or reassessed after completion of PV isolation.

Quantification of CFAE morphology

In previous studies, signal morphology has been characterized based on the following extrinsic features, or parameters, of signal shape[5,6]:

1. Amplitude (scaling along *y*-axis)
2. Time duration (scaling along *x*-axis)
3. Baseline level (shifting along *y*-axis)
4. Phase lag (shifting along *x*-axis)

These features are called *extrinsic* because when signals such as electrograms from successive cardiac cycles are normalized for them, the Cartesian coordinate systems become coincident so that they can be plotted in the same feature space. Once normalized, any remaining differences between the signals are termed *intrinsic*.[5,6] Conditions expected to mostly affect extrinsic morphologic features include the surface area and volume of local tissue that is activating (affecting electrogram amplitude), the conduction velocity (affecting time duration of deflections), the angle and timing of the oncoming wavefront (affecting phase, upstroke and downstroke of deflections), and the influence of electrical activity on the positive versus negative pole of the bipolar recording electrode (affecting baseline level). Conditions expected to mostly affect intrinsic morphologic features include microscopic spatial heterogeneity of remodeling, tissue fibrosis, and refractory period.

Because extrinsic parameters 1–4 are scalar quantities (i.e., they are single values), they are useful for comparing electrograms while minimizing measurement complexity. We previously calculated extrinsic parameters 3 and 4 for electrograms obtained during nonfibrillating rhythms by segmenting according to cardiac cycle.[6] However, CFAE acquired during fibrillation cannot be segmented by cardiac cycle. Instead, individual signal deflections in CFAE obtained during AF were characterized using the phase plot method from nonlinear dynamics. Phase plots are graphs of y_{i+1} versus y_i, where y is a discrete sample point in the digitized signal. Each signal deflection forms a loop, or orbit, in phase space. Figure 1 is an illustrative example of this process, using simulated signals and their phase diagrams. The triangle wave (A) is repetitive, and its phase plot (B) consists of multiple overlapping loops. The phase diagram is a plot of y_{i+1} versus y_i for all y. The periodic signal in Figure 1A is sampled in discrete time as shown. Point 1 in panel A with value −3 and point 2 with value −2 are plotted in (y_i, y_{i+1}) space as the point 1–2 in panel B. This is repeated for subsequent points in the signal. When the periodic signal completes one period (12–1 in panel A), it then begins a new period (panel A) and a new loop in the phase plot (which are overlapped, panel B). Peak amplitude (a), upstroke (b), downstroke (c), and width (d) are labeled for one cycle in panels A and B, with the width of a deflection being represented as one complete orbit in panel B, analogous to shape parameter 2 above. An illustrative example of the influence of random noise added to a simulated electrogram signal is shown in panels C–F. Each of three peak types in panel C overlap with other instances of the same peak type as a distinct loop in the phase diagram (D). If random noise is added (E), the loops representing each particular type of deflection do not precisely overlap (F). Differences in the degree of overlap of the loops represent differences in the intrinsic morphology of each electrogram deflection.

The phase plot loops can be quantitatively characterized, to a first approximation, by the diagonal crossings and the extension of the limbs from the diagonal. For signals with isoelectric intervals between peaks such as those in Figure 1, panels C–F, the diagonal crossing furthest from the origin (y_1,y_2) = (0,0) in the positive or negative direction for each loop (Figure 1D) is representative of peak amplitude (α, β, δ), analogous to parameter 1. The upslope and downslope of each deflection define the *x-y* position of the upstroke l_1 and downstroke l_2, analogous to parameters 3 and 4 (described in greater detail in the Appendix). The extrinsic morphology of CFAE was thus characterized by detecting all

electrogram deflections and measuring peak amplitude, width, and upslope and downslope of each deflection, as described in detail in the Online Supplement. The coefficient of variation (SD/mean) in each CFAE sequence was tabulated for all extrinsic parameters.

Another method was devised to gauge intrinsic CFAE morphology, the point-by-point structure of the signal after normalization to a common feature space.[5,6] We chose to quantify the voltage profile as a measure of intrinsic shape. First, all CFAE sequences were normalized along the *y*-axis by adjusting them to mean zero and unity power, thereby removing *y*-axis extrinsic shape differences. Then the sum of absolute values for all points was determined in each normalized CFAE sequence. This procedure can be expressed mathematically as follows. Suppose a sequence $\underline{y}$ consists of signal sample points with voltage levels of $y_1, y_2, \ldots, y_N$. The energy and power in $\underline{y}$ are given by Equations 1 and 2:

$$E=\sum y_i^2 \quad (1)$$

$$P=1/N \sum y_i^2 \quad (2)$$

where N = 8,192 is the sequence length used in our study (8.4 seconds). The sequences all are set to mean zero and unity power. Because the sequences are set to mean zero, the power is also the signal variance; thus, the standard deviations of all sequences will be identical (squared standard deviation = variance). Now the sum of absolute values is given by Equation 3:

$$|\bullet|=1/N \sum |y_i| \quad (3)$$

To maximize |●|, the derivative is obtained and set to zero:

$$0=d|y_1|+d|y_2|+\ldots+d|y_n|=\sum d|y_i| \quad (4)$$

where the summation order in Equation 4 is unimportant. A solution to this equation occurs when the derivatives are all zero, that is, $|y_i|$ are all the same value. This is illustrated schematically in Figure 2, where the deflections have been normalized to zero mean and 8 mv^2 total energy. The sum of absolute values |●| of the deflections are shown for each sequence. The sum is greatest in panel A, where the peaks are uniform in amplitude. As the peaks become less uniform (B–D), the sum of absolute values decreases, even though the total energy is the same. Although the peaks are depicted as blocks with vertical (infinite) upslope and downslope, the sum of absolute values would similarly be reduced if the upstrokes and downstrokes were more gradual. Thus, CFAEs with uniform sharp peaks have a higher sum of absolute values, whereas CFAEs with meandering deflections have a lower sum of absolute values. Because this method accounts for the voltage profile of all points in the sequence and is not a normalization procedure, it is a measure of the signal structure itself and thus of the intrinsic shape. Although other measures could be devised to measure intrinsic electrogram shape, absolute value analysis has the advantage of simplicity and of being a scalar quantity, which is readily comparable to other measures.

These quantifiers of fractionation were compared to a standard approach of calculating the mean interval between CFAE positive and negative deflections. All three quantifiers (intrinsic and extrinsic CFAE shape, and mean deflection interval) were computer automated and thus were not subject to observer bias. To investigate whether extrinsic or intrinsic signal shape may be dependent upon the frequency of activation, the quantifiers were correlated to the dominant frequency[7] using the Pearson product moment statistical function. The fit of each curve to a straight line was done using linear regression analysis (SigmaPlot version 9.01, 2004. Systat Software, Inc., Chicago, IL). Student's unpaired t-test was used to determine the significance between mean values (P <.05; MedCalc version 9.5.2.0, 2008. MedCalc software, Mariakerke, Belgium).

Results

The CFAE signals shown in Figure 3 were acquired from the ostium of the RSPV in a patient with paroxysmal AF and another patient with persistent AF. The signals appear similar on visual inspection, and neither shows a clear isoelectric line. However, in the phase plots (right) the orbits of the persistent AF signal extend further along the diagonal and further away from the diagonal, indicating larger peak amplitude and faster upstroke and downstroke. The largest peaks are numbered at left (panels A and C), and corresponding orbits are numbered in phase diagrams at right (panels B and D). The peaks of the paroxysmal AF signal (panel A) form only two distinctive loops extending along the diagonal (panel B). This signal would be considered heterogeneous because there is no evident repetitiveness to the deflections of the signal as manifested by the lack of distinctive, clearly demarcated loops in the phase plot. However, there is a single sharp peak that causes a large deviation from the diagonal (arrow in panels A and B). In contrast, the persistent AF signal contains a number of distinctive large peaks of similar positive and negative amplitude (panel C). These particular deflections are manifested in the phase plot as shown (panel D), with many individual deflections being distinguishable. Some of these deflections have similar orbits, and there is additional repetitive lower-amplitude detail (orbits looping around other larger white spaces in panel D); therefore, the signal of panel C would be considered to be more homogeneous compared with the signal of panel A.

Differences in CFAE morphology in paroxysmal and persistent AF

Figure 4 shows the summary plots for the coefficient of variation measurement for amplitude, upslope, downslope, and width (extrinsic morphology parameters) for CFAEs recorded at the ostia of the four PVs and at the posterior and anterior left atrial free-wall sites for the first and the second 8-second CFAE sequences. There was no significant difference in the average value of any of the parameters from the first 8-second recording period compared to the second 8-second sequence, demonstrating the short-term temporal reproducibility of these metrics at all recording sites. The peak amplitude coefficient of variation was highest around the ostium of the RIPV for both paroxysmal and longstanding AF, showing that the greatest dispersion in the CFAE component peak amplitude occurred in this anatomic region for both types of AF (upper left panel). For longstanding persistent AF, the peak amplitude coefficient of variation around the ostium of the RIPV was significantly higher compared to the mean value of the other PVs (P = .008) and was

significantly higher compared to the posterior and anterior left atrial free wall amplitude coefficients of variation (P <.001). The width coefficient of variation was at a minimum at the RSPV ostium indicating the least amount of dispersion in CFAE component width at this anatomic region (lower right panel). Compared to the other veins, the coefficient of variation of the width of CFAE deflections at the RSPV was significantly shorter in paroxysmal (P <.001) as well as long-standing AF (P = .005).

In Figure 5, the summary plot for the absolute value function measurement (intrinsic signal shape) is shown for the same CFAE signals and recording locations as shown in Figure 4. The short-term reproducibility was high for this parameter, as it was for the extrinsic shape measures. In Figure 5, the ordinate axis is inverted so that greater fractionation dispersion (increased variability in the peak voltage levels of CFAE deflections) is upward along the ordinate axis. The sum of absolute values was minimal at the RIPV ostium for persistent long-standing AF and minimal at the LSPV ostium for paroxysmal AF, where minima are toward the top in the graph. As with the coefficient of variation measurements of Figure 4, at each anatomic location, paroxysmal CFAEs have greater disparity compared with persistent CFAE signals as expressed by the lesser sum of absolute values (toward top in graph).

Both extrinsic (Figure 4) and intrinsic (Figure 5) shape measurements had greater variability in paroxysmal compared with persistent AF. Thus, CFAE deflections tended to be more nonuniform and heterogeneous during acutely induced AF in patients with clinical paroxysmal AF compared with long-standing persistent AF. The significance of these differences for both extrinsic and intrinsic parameters is depicted in Table 2. For the coefficient of variation of extrinsic parameters (peak amplitude, upslope and down-slope, peak width), the greatest significance of the differences occurred at the LSPV, followed by the posterior left atrial free wall and RSPV, anterior left atrial free wall, and LIPV, and finally by the RIPV, where only the coefficient of variation of the width parameter was significantly different. For the intrinsic parameter (sum of absolute values), significant differences occurred only at the LSPV and RSPV ostial recording sites. The significance of the differences for mean CFAE deflection intervals in paroxysmal versus persistent AF are depicted in Table 3, with actual values also shown. As in Table 2, the LSPV and POS locations have the most significant difference, but these are only moderately significant (P <.05). Thus, the extrinsic parameters have greater resolving capacity based on AF type (Table 2) compared with the traditional measure used to characterize CFAE (Table 3).

Correlation between frequency of activation and CFAE morphology

A possible effect of atrial tissue activation rate on dispersion in CFAE parameters was investigated. Both extrinsic and intrinsic morphology measurements were not well correlated to dominant frequency (mean absolute value of r^2: 0.19, maximum: 0.32); therefore, these measures are robust to patient-to-patient differences in activation rate (see Online Supplement for more details).

Discussion

This study compared the degree of heterogeneity of CFAE components recorded during acutely induced AF in patients with paroxysmal AF and those recorded during long-standing AF. The methods used for quantifying CFAE complexity included the coefficient of variation function based on nonlinear dynamic theory, using the elements of the phase plot to describe the syntactic structure of the signal (extrinsic morphology), and the sum of absolute values, which compares all of the individual sample points of the signal after normalizing for power (intrinsic morphology). Our results show that significant differences exist in CFAE patterns, especially in those recorded at the LSPV and posterior left atrial free wall, between acutely induced and longstanding persistent AF, and that these are not likely to be due solely to differences in the frequency of local atrial tissue activation.

Electrogram fractionation and AF substrate

The extrinsic and intrinsic shape measurements that we devised in this study do not count the number of peaks per unit time; rather, they measure the variation in peak shape and include all peaks in the calculation. Therefore, dispersion of fractionation is calculated in terms of repetition. Heterogeneity in fractionation in this sense is a lack of repetition in the activation pattern as manifested in peak shape. Repetition and periodicity, no matter on how small a level, result in a low fractionation score (low morphometric coefficient of variation and high sum of absolute values). Such differences in the pattern of fractionation in turn may reflect the differences in pathophysiology of one type of AF versus another. The pathogenesis of long-standing AF involves complex, time-varying alterations at the cellular and tissue levels. Electrogram fractionation may occur in regions of low atrial voltage, shortened refractory periods, and decreased conduction velocity, resulting in microreentry. One then would expect more homogenous and repeating CFAE patterns. However, even in the absence of such structural changes, CFAEs may be observed due to irregular activation patterns that are recorded in acute experimental preparations and in patients with paroxysmal AF, who lack structural heart disease and have sinus rhythm most of the time. Wavebreaks and changes in the direction of activation as a result of changing refractoriness in the tissue surrounding rotors or high-frequency activation areas may cause increasingly fractionated electrogram morphology in otherwise normal tissue architecture. One then would expect more heterogeneous and nonrepeating CFAE patterns.

Clinical implications

It has previously been shown that ectopic beats preceding the onset of paroxysmal AF originate commonly in the PVs.[8] In this seminal study, 94% of the triggers were found in the PVs, and 48% of these triggers occurred in the LSPV, 26% in the RSPV, 17% in the LIPV, and only 9% in the RIPV.[8] The site-specific prevalence for these ectopic foci approximately parallel the significant differences in morphologic parameters in paroxysmal versus persistent AF patients in our study. The greatest difference in electrogram morphology occurred at the ostia of the LSPV (Table 2). By comparison, only two morphologic parameters were significantly different at the RIPV (Table 2). If the drivers of paroxysmal AF originate most frequently in or at the ostium of the LSPV, then one would expect the greatest changes in electrogram morphology as caused by nearby wavebreaks to occur

around the LSPV ostia and the least around the RIPV ostia. Table 2 shows that this is exactly the case for acute AF compared to long-standing AF, where the extent of remodeling is likely to be relatively large. Another location identified by our methods as manifesting high heterogeneity in CFAE components was the posterior left atrial wall. In previous studies, the data for the role of the left atrial posterior wall in harboring AF triggers is more experimental than clinical.[9]

Targeting CFAEs as an ablation strategy aims to remove the substrate for AF, assuming that CFAEs represent electrical phenomena closely associated with arrhythmogenic substrate.[3] Modest short-term efficacy has been achieved by catheter ablation of persistent AF guided by CFAE sites, but only after a second ablation procedure in >40% of patients.[10] Even less clear is whether targeting of CFAEs in paroxysmal AF has any additional effect on long-term results.[3] If CFAEs associated with greater morphologic variability as observed in patients with paroxysmal AF in our study represent wavebreak sites at the periphery of the sources,[9] one would expect them to be less effective as ablation targets. In contrast, if CFAEs with low morphologic variability represent electrophysiologic phenomenon occurring within the arrhythmogenic sites, such as microreentry, they would be more suitable targets for ablation. In either case, accurate quantification of signal morphology is a rational first step in locating such candidate areas, and our results show the feasibility of such distinction. (Discussion is continued in the Online Supplement.)

Supplementary Material

Refer to Web version on PubMed Central for supplementary material.

ABBREVIATIONS

AF	atrial fibrillation
CFAE	complex fractionated atrial electrogram
LIPV	left inferior pulmonary vein
LSPV	left superior pulmonary vein
RIPV	right inferior pulmonary vein
RSPV	right superior pulmonary vein

References

1. Stiles MK, Brooks AG, Sanders P. Putting CFAE on the map. J Cardiovasc Electrophysiol. 2008; 19:904–906. [PubMed: 18554198]
2. Nademanee K, McKenzie J, Kosar E, et al. A new approach for catheter ablation of atrial fibrillation: mapping of the electrophysiologic substrate. J Am Coll Cardiol. 2004; 43:2044–2053. [PubMed: 15172410]
3. Porter M, Spear W, Akar JG, et al. Prospective study of atrial fibrillation termination during ablation guided by automated detection of fractionated electrograms. J Cardiovasc Electrophysiol. 2008; 19:613–620. [PubMed: 18462320]

4. Jaïs P, Haïssaguerre M, Shah DC, Chouairi S, Clémenty J. Regional disparities of endocardial atrial activation in paroxysmal atrial fibrillation. Pacing Clin Electrophysiol. 1996; 11(Pt 2):1998–2003. [PubMed: 8945085]
5. Widrow B. Rubber-mask technique 1. Pattern measurement and analysis. Pattern Recognit. 1973; 5:175–197.
6. Ciaccio EJ, Scheinman MM, Fridman V, Schmitt H, Coromilas J, Wit AL. Dynamic changes in electrogram morphology at functional lines of block in reentrant circuits during ventricular tachycardia in the infarcted canine heart: a new method to localize reentrant circuits from electrogram features using adaptive template matching. J Cardiovasc Electrophysiol. 1999; 10:194–213. [PubMed: 10090223]
7. Ciaccio EJ, Biviano AB, Whang W, Wit AL, Coromilas J, Garan H. Optimized measurement of activation rate at left atrial sites with complex fractionated electrograms during atrial fibrillation. J Cardiovasc Electrophysiol. 2010; 21:133–143. [PubMed: 19793138]
8. Haissaguerre M, Jais P, Shah DC, et al. Spontaneous initiation of atrial fibrillation by ectopic beats originating in the pulmonary veins. N Engl J Med. 1998; 339:659–666. [PubMed: 9725923]
9. Zlochiver S, Yamazaki M, Kalifa J, Berenfeld O. Rotor meandering contributes to irregularity in electrograms during atrial fibrillation. Heart Rhythm. 2008; 5:846–854. [PubMed: 18534369]
10. Oral H, Chugh A, Good E, et al. Radiofrequency catheter ablation of chronic atrial fibrillation guided by complex electrograms. Circulation. 2007; 115:2606–2612. [PubMed: 17502567]

Appendix

Suppose that a CFAE signal deflection has an upstroke that monotonically increases and a downstroke that monotonically decreases along the *y*-axis. The slope, or derivative, of the upstroke and downstroke determines the distance from diagonal to right and left orbital limbs in the phase plot (Figure 1, panels C and D, l_1 and l_2). The upstroke and downstroke components can each be described mathematically as Equation A1:

$$\begin{aligned} y(x) &= \int (dy/dx)\, dx \approx \sum (\Delta y/\Delta x)\Delta x + c_2 \\ &= \sum \Delta y + c_2 \end{aligned} \quad \text{(A1)}$$

where y is amplitude (voltage), x is sample number, dy/dx is slope (derivative), and c_2 is the reference point. Supposing a monotonic change in upstroke and in downstroke, it is also valid to write Equation A2:

$$\begin{aligned} x(y) &= \int (dx/dy)\, dy \approx \sum (\Delta x/\Delta y)\Delta y + c_1 \\ &= \sum \Delta x + c_1 \end{aligned} \quad \text{(A2)}$$

From Equations A1 and A2, the position of both upstroke and downstroke can each be described as the sum of incremental changes Δx and Δy, referenced to fiduciary point (c_1,c_2), which is taken as the peak amplitude location. If, to a first approximation, both upslope and downslope are constants, then

$$x = (dx/dy)(y - c_2) + c_1 \quad \text{(A3)}$$

$$y = (dy/dx)(x - c_1) + c_2 \quad \text{(A4)}$$

where (x,y) is the position of the upstroke or downstroke. Supposing upslope, downslope, and peak amplitude are measured, then for both upstroke and downstroke the x position is pinned by the y position and vice versa.

Appendix

Supplementary data

Supplementary data associated with this article can be found, in the online version, at doi: 10.1016/j.hrthm. 2010.06.018.

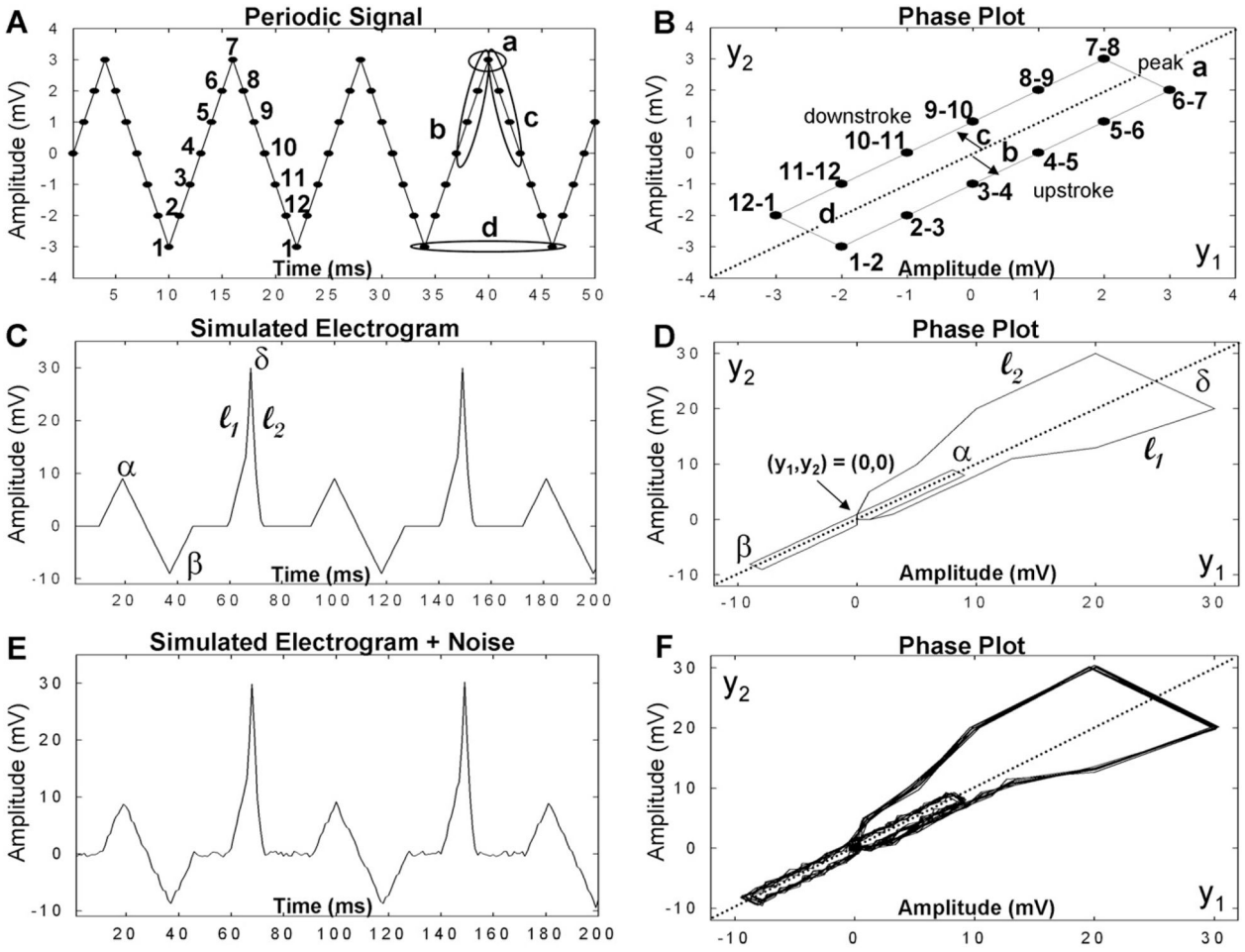

Figure 1.

Phase plot descriptions. **Left panels:** Simulated signals varying in amplitude over time. **Right panels:** Corresponding phase plots for these signals.

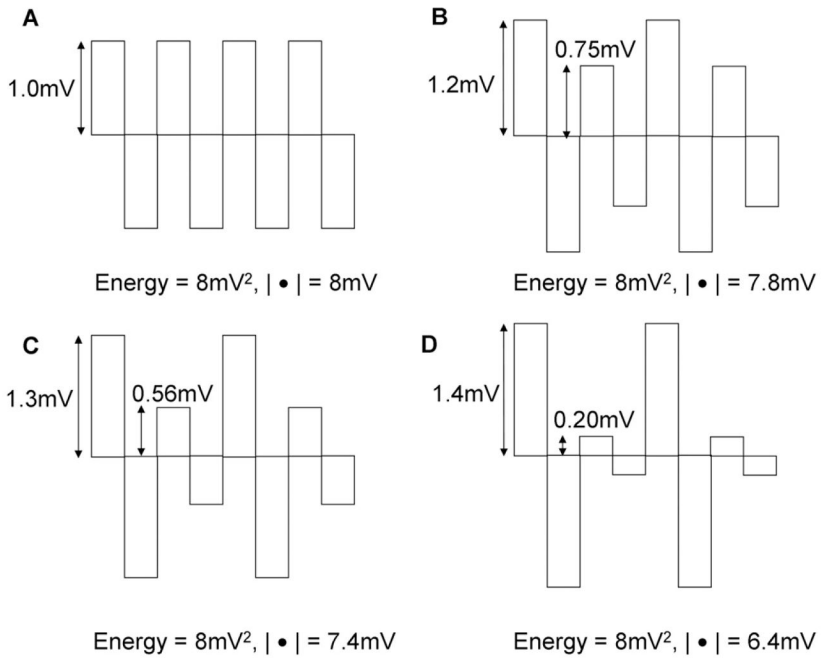

Figure 2.

Schematic diagrams showing positive and negative rectangular pulses with increasing disparity in amplitude but constant power and energy from **A** to **D.**

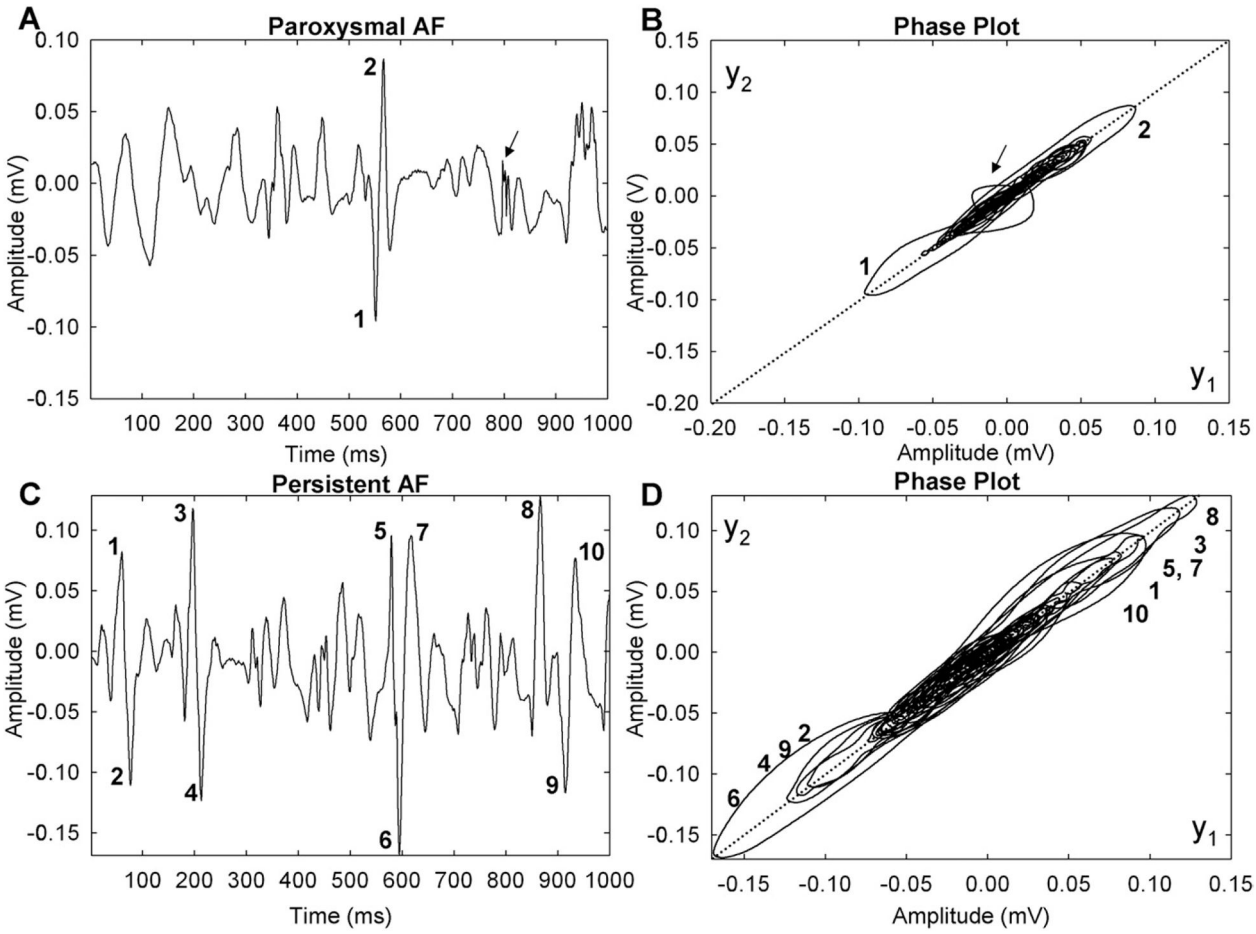

Figure 3.

Signals and phase plots from paroxysmal **(A, B)** and long-standing persistent **(C, D)** atrial fibrillation (AF).

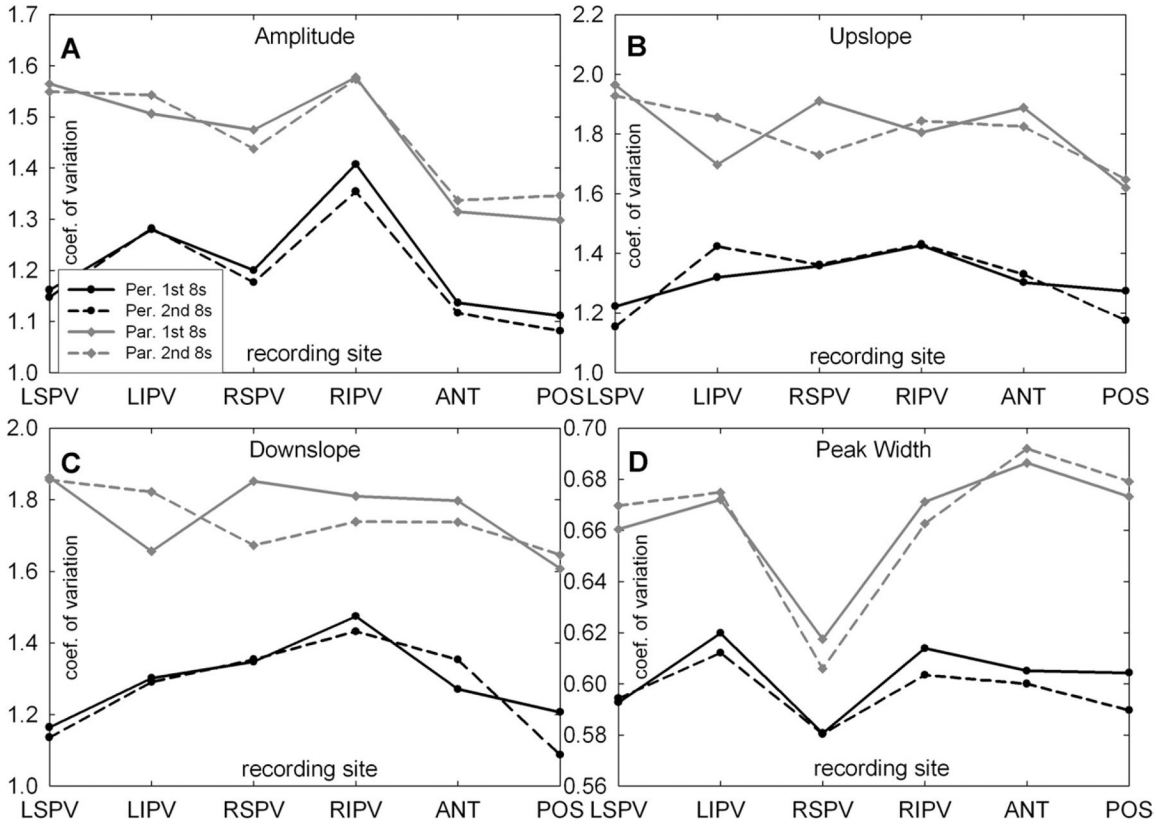

Figure 4.

Summary plots of the coefficient of variation (COV) for the four different complex fractionated atrial electrogram morphologic parameters (amplitude, upslope, downslope, and peak width) for paroxysmal and long-standing atrial fibrillation. ANT = anterior left atrial free wall; **LIPV** = left inferior pulmonary vein; **LSPV** = left superior pulmonary vein; POST = posterior left atrial free wall; **RIPV** = right inferior pulmonary vein; **RSPV** = right superior pulmonary vein.

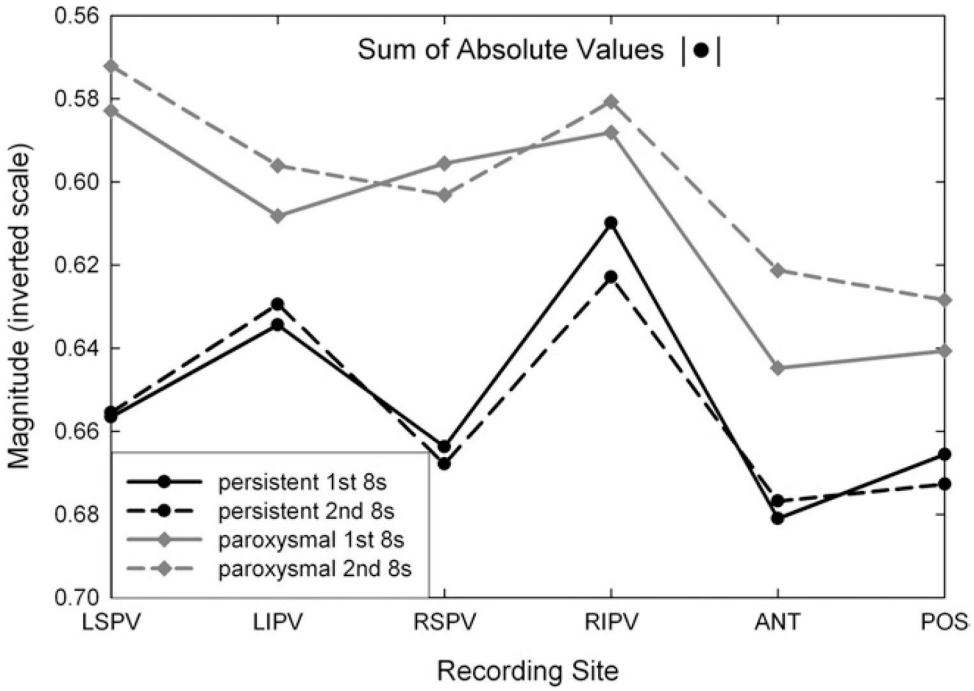

Figure 5.

Plots of mean sum of absolute values measured in complex fractionated atrial electrograms recorded from different anatomic sites. ANT = anterior left atrial free wall; **LIPV** = left inferior pulmonary vein; **LSPV** = left superior pulmonary vein; POST = posterior left atrial free wall; **RIPV** = right inferior pulmonary vein; **RSPV** = right superior pulmonary vein.

Table 1

Clinical patient data

AF type	Age (years)	Duration† (years)	Coronary artery disease (n)	Hypertension (n)	Left atrial diameter* (cm)	Left ventricular end-diastolic diameter (cm)	Left ventricular ejection fraction (%)	Mild mitral regurgitation (n)	Left ventricular wall thickness (cm)
Paroxysmal	61.5 ± 9.6	1–16	1/10	3/10	4.23 ± 0.42	4.99 ± 0.43	60.5 ± 6.2	2/10	1.21 ± 0.07
Persistent	55.7 ± 7.1	1–9	0/10	6/10	4.84 ± 0.55	5.05 ± 0.63	56.8 ± 4.6	3/10	1.26 ± 0.38

*Difference in diameters is significantly different (P <.02).

†For paroxysmal atrial fibrillation (AF), duration represents the time from onset of first symptom attributable to AF to the time of catheter ablation. For persistent AF, the duration represents the period of uninterrupted AF up to the day of catheter ablation. See text for details.

Table 2

Significant differences in fractionation parameters for paroxysmal versus persistent atrial fibrillation

Parameter	LSPV	LIPV	RSPV	RIPV	ANT	POS
amp-1st 8s	**	—	*	—	—	*
upsl-1st_8s	**	*	*	—	*	*
dnsl-1st_8s	**	*	*	—	*	*
wid-1st_8s	**	—	*	*	*	*
amp-2nd_8s	**	—	*	—	—	*
upsl-2nd_8s	**	*	*	—	*	*
dnsl-2nd_8s	**	**	—	—	—	**
wid-2nd_8s	**	*	—	*	**	**
abs-1st_8s	*	—	*	—	—	—
abs-2nd_8s	*	—	*	—	—	—

1st, 2nd = values during first and second 8-second recording period, respectively; abs = absolute value; amp = peak amplitude; ANT = anterior left atrial free wall; dnsl = downslope; LIPV = left inferior pulmonary vein; LSPV = left superior pulmonary vein; POST = posterior left atrial free wall; RIPV = right inferior pulmonary vein; RSPV = right superior pulmonary vein; upsl = upslope; wid = width.

* $P < .05$;

** $P < .001$;

— = not significant.

Table 3

Means and significant differences in deflection intervals for paroxysmal versus persistent atrial fibrillation

Parameter	LSPV	LIPV	RSPV	RIPV	ANT	POS
MN-1st_8s	17.02_18.72	17.81_18.37	17.75_17.67	16.81_18.58	19.06_22.06	18.16_20.99
MN-2nd_8s	16.83_18.79	17.70_18.94	17.89_17.58	16.77_18.08	19.23_21.49	18.32_20.95
sig-1st_8s	*	—	—	—	*	*
sig-2nd_8s	*	—	—	—	—	*

MN = mean value of complex fractionated atrial electrogram deflection interval in milliseconds; sig = significance. Other abbreviations as in Table 2. In each column, left side is persistent atrial fibrillation and right side is paroxysmal atrial fibrillation.

* $P < .05$;

— not significant.